Comparison of Hydraulic Function and Channel-Floodplain Connectivity Between Actively and Passively Restored Reaches of Stroubles Creek 11 Years After Restoration

Nicholas Christensen

Thesis submitted to faculty of Virginia Polytechnic Institute and State University in partial fulfillment of the requirements for the degree of

Master of Science in Biological Systems Engineering

Jonathan Czuba, Chair

William C. Hession

Kyle Strom

May 6th, 2022

Blacksburg, VA

Keywords: Stream Restoration, Passive restoration, Stream Hydraulics, Fluvial Geomorphology

Comparison of Hydraulic Function and Channel-Floodplain Connectivity Between Actively and Passively Restored Reaches of Stroubles Creek 11 Years After Restoration

Nicholas Christensen

Abstract

A hydraulic model was developed to determine differences in the hydraulic characteristics of three different reaches of an urban- and agriculturally-impacted stream in southwest Virginia. The three reaches all had cattle excluded from the channel in 2010. The farthest upstream, Treatment 1, was left to progress without intervention beyond cattle removal while the other two, Treatments 2 and 3, were regraded and stabilized using common stream restoration techniques and a forested riparian was established. The banks of Treatment 2 were regraded to a slope of 3:1 while Treatment 3 was designed with a flat inset floodplain cut into the banks. The model results showed that the self-adjustment in Treatment 1 exhibited inset floodplains with diverse topographical structure including floodplain channels. These adjustments provided higher floodplain volume and mass exchange between the channel and the floodplain when compared with the stable, straight Treatment 2. Comparisons between Treatment 1 and Treatment 3 did not clearly show which treatment was more well connected, with some metrics showing Treatment 1 was more connected while others indicated the opposite. Overall, the findings indicate that stabilization of channelized streams without consideration of the natural planform prolongs adjustment to a channel-floodplain form with more exchange of water, sediment, nutrients and providing refuge for biota.

Comparison of Hydraulic Function and Channel-Floodplain Connectivity Between Actively and Passively Restored Reaches of Stroubles Creek 11 Years After Restoration

Nicholas Christensen

Abstract (general audience)

A water flow model was developed to determine differences in between sections with different management practices an urban- and agriculturally-impacted stream in southwest Virginia. The three reaches all had cattle excluded from the channel in 2010. The farthest upstream, Treatment 1, was left to progress without intervention beyond cattle removal while the other two, Treatments 2 and 3, were stabilized by changing the bank slope and planting trees. The banks of Treatment 2 were regraded to a slope of 3:1 while Treatment 3 was designed with a flat section cut into the banks. The model results showed that the self-adjustment in Treatment 1 created an bench similar to Treatment 3. This section flooded more readily and allowed for higher flow of water between the channel and the floodplain when compared with the stable, straight Treatment 2. Comparisons between Treatment 1 and Treatment 3 did not clearly show which treatment was more well connected, with some metrics showing Treatment 1 was more connected while others indicated the opposite. Overall, the findings indicate that stabilization of channelized streams in their man altered state prolongs adjustment to a more natural form which provides services including flood mitigation, sediment cycling, nutrient cycling and habitat for plants and animals in and along the stream.

Acknowledgements

Thank you to **Jon Czuba** for introducing me to the research world, your mentorship in my personal and professional life, and continuing to challenge and inspire me to do more. Thank you to **W. Cully Hession** for your hard work creating and maintaining StREAM Lab, and your guidance helping me to become a better teacher and communicator. Thank you to **Kyle Strom** for teaching me so much about hydraulics and sediment transport and making the astounding limits in our collective understanding clear and exciting. Thank you to **Beth Prior** for her help and guidance in creation of the DEM used in this research and for being patient and available as I found my place on our research team. Thank you to **Tess Thompson** for introducing me to the intricacies of stream restoration and pushing me to understand underlying principles and data informing our management. Thank you to **Case Davis, Chuck Davis,** and **Brian Belcher** for giving me the perspective of practitioners and inspiring me to dig deeper into what makes a design successful. Thank you to **Sierra Smith** for keeping me excited about my work and always being open to discussing the work of our group. Last but certainly not least, thank you to **Diana Schmidt** for her endless support and reassurance when my research was overwhelming and seemingly impossible.

Contents

List of figures

Introduction

The ability of a river to exchange water, sediment, and nutrients with its floodplain at high flows is referred to as channel-floodplain connectivity. Channel-floodplain connectivity has been quantified with multiple metrics rooted in hydraulic modeling. Perhaps the most basic form of quantification comes from looking at the flood extents and floodplain water depth (Czuba et al. 2019, Hammersmark 2008). This approach is expanded upon by looking specifically at exchanges of mass and momentum between a channel and its floodplain (Byrne 2019, Czuba 2019). Examining exchanges of mass and momentum allows for insight into biogeochemical processes and flood propogation. Researchers have explored channel-floodplain interactions with a channel length normalized flux of water to allow for comparison of the degree of connectivity between systems (Byrne 2019, Czuba 2019). By comparing the degree of channel-floodplain connectivity of river systems, we can also determine the relative differences in floodplain services between systems (Hammersmark 2008).

Significant alterations have been made to stream channels to contain flows within the channel thus reducing channel-floodplain connectivity (Bernhardt 2005). Among these alterations are channelization, levee building, wetland drainage, and damming. Of particular importance in headwater streams is the practice of channelization which often involves straightening, widening, and deepening to increase the streams capacity and contain flow in the channel (Bernhardt 2005). The new efficient channel quickly moves water through the landscape without interacting with the floodplain. This reduction in channel-floodplain connectivity has had unforeseen consequences including significant damage to natural stream

structure, stream ecosystems, and a lack of flood dissipation leading to larger floods downstream (McMillan 2017).

Stream restoration is often used as a tool to revert channelized streams to a state which has higher channel-floodplain connectivity (Bernhardt 2005, Hammersmark 2008). These changes are often aimed at enhancing aquatic habitat, dissipating flood-flow energy, decreasing peak flows, and reducing bank erosion (Bernhardt 2005, McMillan 2017). Channel-floodplain connectivity is often restored by reworking of the stream channel, herein referred to as active restoration. Active restoration aims to accelerate the evolution of the channel geometry into a dynamic equilibrium which would theoretically be reached given enough time for channel adjustment (Levell 2008). The adjustments made in active restoration are expensive and can damage the biological community short-term by clear cutting and soil compaction (Bernhardt 2005, Bernhardt 2011, Laub 2013). There has been a call for the past several years to move away from active regrading projects towards more efforts to influence river processes through less invasive management processes (Bernhardt 2011, Wohl 2015). Passive forms of restoration including cattle exclusion and planting woody riparian zones have also been implemented to influence channel form and uplift local ecosystems (Trimble 1994, Bernhardt 2011).

How we define the success of a restoration project is an active field of study. There are multiple aspects of stream systems which we hope to affect with restoration practices including the geomorphic stability, hydraulic performance, and biological integrity (Bernhardt 2005). Monitoring of restored sites has been harshly criticized for its short study time and limited parameters of investigation (Wohl 2015, Rubin 2017). Monitoring for geomorphic stability and biological integrity is standardized and mostly relies on repeated surveys of stream geometry,

woody vegetation, and benthic macroinvertebrate populations (Bernhardt 2005). Quantifying hydraulic properties is less standardized and less common in the world of practitioners, but has been accomplished by some researchers (Hammersmark 2008, Bernhardt 2011).

Previous studies have explored channel floodplain connectivity and the associated services it provides in restored streams. Hammersmark et al. (2008) modeled the pre- and post-restoration forms of a fully regraded stream and found increased floodplain inundation with the same magnitude storm. Sholtes (2009) builds on this work by modeling the flood wave propogation in a simulated restoration project, finding that the wave was damped by the restoration project. These studies indicate that the regraded channels provide higher channel-floodplain connectivity and their associated services immediately after construction. McMillan et al. (2017) adds to this by quantifying the sedimentation and nutrient cycling of restored channels of different ages but does not compare them to pre-restoration conditions or similar systems which have been passively restored.

Previous research is missing direct comparisons of channel-floodplain connectivity and associated services between active and passive restoration projects and how these services change as streams adjust after restoration. This project is the first known direct comparison of channel-floodplain connectivity between actively and passively restored treatments of the same stream. Additionally, this project examines the influence of time on the hydraulic function of a restored stream restoration with data 11 years after restoration. Understanding the hydraulic differences between actively and passively restored reaches is of the utmost importance when practitioners are highly incentivized to implement streambank regrading projects (Wohl 2015). We aim to fill this gap in our understanding using direct comparison of

the hydraulic characteristics in streams with common regrading treatments and a naturally adjusting stream reach. In doing so we aim to influence the discussion on design and regulation of restored streams to promote more effective stream restoration which better achieves our goals of floodplain reconnection.

Methods

Site Description:

The study site is a managed reach of Stroubles Creek in Blacksburg VA called the StREAM Lab (Figure 1). The stream is in the Valley and Ridge physiographic province of Virginia. The contributing watershed is highly urbanized with 81 % urban land cover. The studied reach of stream has a 1,530 ha drainage area, 0.22 % slope, and sinuosity of 1.1. The floodplain around the stream has been designated as a research area and is vegetated with a mix of short trees, shrubs, and grasses. A mowed path is maintained within the floodplain to provide access for equipment maintenance. The hillslope has cultivated crops on the Southeast side of the stream and a cow pasture on the Northwest. The cow pasture extended into the stream untill 2010 when a stream restoration project called for the removal of the cattle. Dominant soils in the floodplain are McGary and Purdy soils which are deep soils (~2 m to restrictive layer) characterized by high clay content and slightly poor drainage.

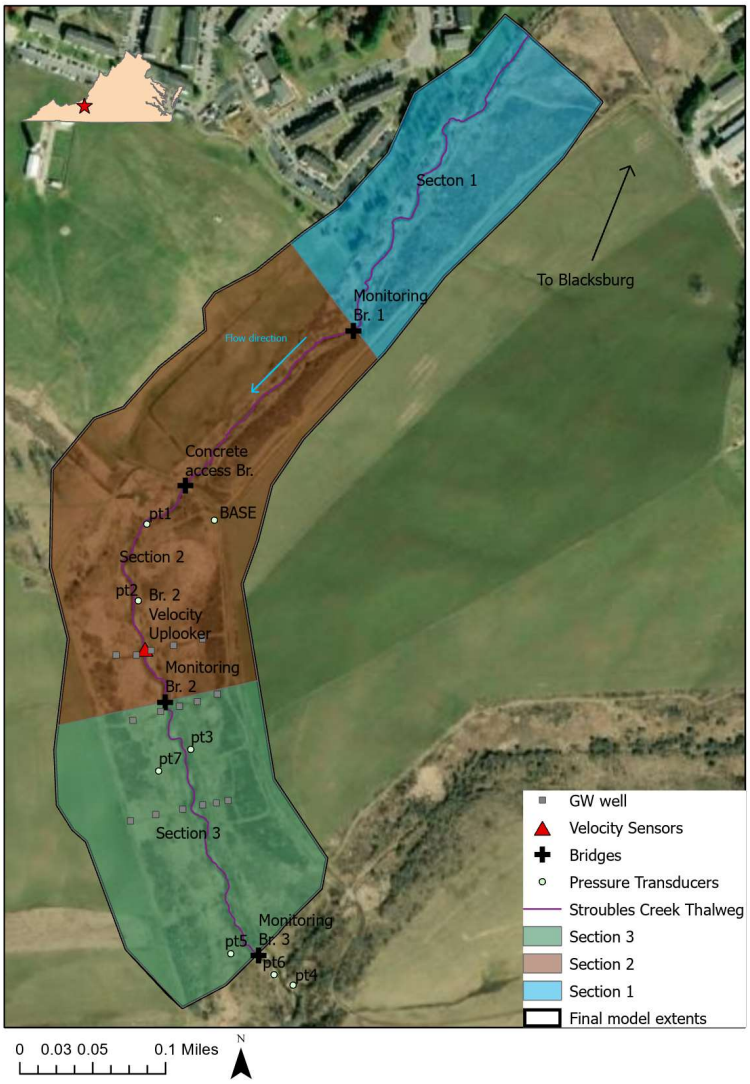

Figure 1: Study area, delineates the treatments of restoration and identifies the locations of relevant instrumentation.

The site was designated as impaired in 1996 due to an excess of fine sediment loading. A stream restoration project was implemented in 2010 with a goal to reduce sediment loading from bank erosion (Thompson et al., 2010). This restoration utilized three different restoration techniques in three separate stream reaches. These reaches of the site will be referred to as Treatments 1, 2, and 3 with treatment number increasing moving downstream as pictured in

figure 1. Treatment 1 (valley length 480 m) was passively restored by removing cattle only. The two reaches downstream (510 m and 300 m) were actively restored. These actively restored treatments of the stream were regraded and replanted with native vegetation to promote stability. The banks of Treatment 2 were regraded from nearly vertical to a 3:1 slope. Treatment 3 had the banks set to the same slope but left a flat inset floodplain between the baseflow channel and the upper floodplain. The restoration along Stroubles Creek allowed for a direct comparison of the channel-floodplain connectivity between actively and passively restored treatments of the same stream. Regrading efforts were focused entirely on changing cross sectional geometry with no changes to longitudinal and planform geometry. Treatment 1 has the highest slope at 0.30% and the highest sinuosity at 1.15. Treatment 2 has a slower slope and sinuosity at 0.20% and 1.05, respectively. Finally, Treatment 3 has intermediate values between Treatments 1 and 2 with slope and sinuosity of 0.25% and 1.13, respectively.

The site is instrumented to collect hydrologic, water quality and hydraulic data to characterize the site. Stage has been measured with pressure transducers for over 10 years at 15-minute increments at Bridges 1 and 2. Additionally, there are 4 in-situ uplooking acoustic doppler current profilers (ADCPs) two of which have been recording data since 2019 and the other two since 2021, averaging velocities over a 2-min period and recording every 5 min.

Model Geometry

A hydraulic model was developed in HEC-RAS 2-D. A Digital Elevation Model (DEM) was created by combining drone lidar data and surveyed bathymetry. Lidar data was taken using a Vapor35 (AeroVironment, Simi Valley, CA, USA) equipped with a YellowScan Surveyor Core lidar system (Monfeerier-sur-Lez, France). Two flights on November 17th and December 10th were

completed to capture the entire study area due to limited drone battery life. Lidar post processing was completed using the CloudCompare software, where lidar points were aligned with surveyed points of the concrete bridge. The processed point cloud was then converted into a raster DEM. The bathymetric survey was conducted using a Trimble R12 GNSS System (Trimble, Sunnyvale, CA, US) from mid-November to December 2022. Cross sections were measured from top of bank to top of bank measuring a minimum of points on the top of each bank, toe of each bank and at the thalweg. Cross sections were spaced at approximately every 7 m (two channel widths). A higher density of cross sections was measured in areas of rapid bathymetric change to best capture the geometry of the stream. GPS data were post-processed using the OPUS correction from NOAA on the base station location (NOAA 2021). After this correction was complete, all cross sections were plotted along their nearest upstream and downstream neighboring sections and visually inspected for quality control. A DEM was then created from the bathymetric points, excluding the top of bank points using ArcGIS function "Raster from Topo" which interpolates between the measured data points in 2D space creating a representation of the topography with 0.1 m cells. The interpolated bathymetric DEM was then clipped based on the extent of the water surface at the time of the lidar flight, which was determined visually from the lidar DEM. The lidar based DEM and bathymetry were then mosaiced into one DEM using ArcGIS' "Mosaic to new raster" with the preference for the bathymetric DEM where data overlapped.

Four bridges fell within the boundary of the model. The bridges were modeled as only abutments with the deck omitted from the model as there is not currently functionality in HEC-RAS 2D to model bridges. During modeling it was determined that the extent of the 0.1 m lidar

was not sufficient to allow for simulation of higher flows. As such a 1 m DEM was obtained from USGS (2021) to extend the model geometry farther up the floodplain. Integration of this 1 m DEM with the existing 0.1 m DEM was completed in RAS-Mapper as it allows for tools to create terrain files which have inconsistent cell spacing. Where data overlapped, the 0.1 m DEM was preferred.

The mesh created for 2D flow simulation was divided into two areas with an area with finer spacing in the main corridor of flow and a coarser floodplain spacing. The inner, finer area was constrained to the base flow channel and the low (inset) floodplain. The other area contained the terrace of the upper floodplain out to the hillslopes, which were not inundated by the simulated flows. The spacing was defined with refinement regions in HEC-RAS by visual observation of the DEM underlain with a hillshade. Spacing for the inset floodplain was set to 1 m with additional refinement occurring at the breaklines, which were set at the boundary of the baseflow channel. Spacing was set as finely as possible while maintaining model stability with timesteps of 0.25s for the largest modeled flows. The upper floodplain cell size was set to 2 m, again with the aim of minimizing mesh size while maintaining model stability.

Model Calibration

Model calibration was completed by adjusting Manning's roughness values until the simulated rating curve matched the observed stage-discharge relationship measured by the main channel in-situ velocity sensor. Roughness was set in three different zones, the channel, floodplain, and mowed access path. Initial roughness values were set as 0.04, 0.50 and 0.04 for the channel, floodplain, and access path based on a previous model created by Prior et al. (2021). Roughness values were assumed to be constant with regard to flow depth over the

range of modeled flows. Flows every CMS from 2-12cms were simulated in the model and steady state water-surface elevation (WSE) was recorded for each simulated flow. The difference between the model results and the best fit of the velocity sensor were quantified using a root mean square error (RMSE). The best fit developed for the in-channel velocity data was a piecewise function with a break at 4cms. Below 4cms the data followed a linear trend while above it the data followed a power function. Using the RMSE and visual inspections of the data the roughness was iteratively adjusted to best agree with the velocity sensor within its 95% prediction interval.

Model Evaluation

The calibrated model was then used to simulate four observed peak flows ranging from 5.44, 6.82, 7.16 and 10.34cms. This flow range was chosen because flows below 5cms did not inundate many of the pressure transducers reducing the number of data points which could be compared to the modeled WSE. The peak of each event was run until the model reached steady state at which time the WSE profile was exported. This modeled WSE profile was then compared to all collected pressure transducer data from the observed peak. Not all transducers were able to capture every event so the number of observations for each peak varied from 5-9 depending on which transducers were inundated and operational. Observed maximum WSE was plotted along with the modeled WSE, and the RMSE between these observed and simulated data was calculated for each event. All simulated and observed data points were then plotted against each other to better represent the observed error.

Floodplain Characterization

Peak flows from 3-12 cms were simulated using the fully calibrated roughness values. A below 7 cms, steady state values of flows at every 0.25 cms were simulated as small increases in flow lead to large changes in stage. From 7-10 cms flows were simulated every 0.5 cms because larger amounts of flow impacted WSE less. From 10-12 cms the flows at each cms were simulated following the same line of reasoning. In all, at least one simulation for each 5 mm interval of WSE measured at the in-stream velocity sensor. Steady state conditions for each flow were output as text files with hydraulic depth, and two-dimensional velocity at each cell center (Czuba 2019; Worley 2022). Text files were read into MATLAB for further analysis using a script developed by Czuba et. al (2019). Once read into MATLAB, logical and linear algebra techniques were used to extract floodplain volume, floodplain depth, channel-floodplain exchange, floodplain residence time, and flow within the floodplain.

In MATLAB, the irregularly spaced cells were interpolated into a regularly spaced grid to allow for use of MATLAB's built in tools for integration to specified points. These grids of velocity and depth were then multiplied by each other to create a grid of cell unit discharge vectors (m^2/s). Floodplain volume was calculated by multiplying the average depth (m) of all cells contained in the floodplain by the cell area (m^2). Channel exchange was calculated following the approach of Czuba et al. (2019) by interpolating the cell discharge vectors to points generated along each bank, projecting the new discharge vectors onto a unit vector which was perpendicular to the bank and then multiplying by the spacing between the calculation points on the bank (m^3/s). The total flow discharge into the floodplain of each reach was calculated by summing all the positive flow vectors and multiplying by the vector spacing.

An average discharge per meter of stream bank was then calculated by dividing the total flow discharge into the floodplain by the reach length so that exchange in each reach could be directly compared to each other without the bias of reach length. Floodplain residence time was calculated by dividing the volume of water in the floodplain by the sum of all positive flow vectors going into the floodplain. Floodplain volume was normalized by dividing floodplain volume of each treatment by the volume in the channel in that treatment. Flow contained inside the channel at each flow was found by drawing cross sections from bank to bank every 10m and then calculating flow normal to the cross section. The flow within the floodplain for each treatment was calculated by finding the flow within the channel and subtracting it from the flow specified at the boundary condition. This analysis was completed twice to examine how the system changes when we consider the inset floodplain as part of the floodplain or as part of the main channel.

Bed Shear Stress Calculation

Bed shear stress was calculated to compare the bed stability of each treatment. Bed shear for each cell was calculated using a rearrangement of equations 2-18, 2-20 and 2-23b of (Garcia 2008). This derivation begins with the equation for steady state bed shear stress (equation 2-18) calculated from roughness, velocity, and fluid density. The roughness coefficient C_f is then converted to Manning's roughness (n) using equations 2-23b and 2-20. After this substitution, steady state bed shear stress at each cell becomes a function of Mannings roughness, cell depth, fluid density, and the magnitude of velocity. This equation for bed shear stress relies on the assumption that the energy slope is equal to the bed slope and that the energy loss in the fluid is due only to the skin friction imparted by the bed material.

Bed shear stress was calculated where these assumptions are best met; at steady state in the channel where the streambed material is sand and gravel. Floodplain shear stresses are not explored as the calculated floodplain shear stresses includes energy lost to vegetation making this metric less representative of sediment mobilization characteristics than values calculated within the channel. The final equation used to calculate steady state bed shear stress in each cell is below.

Equation 1:

$$\tau_{b,cell} = \frac{\rho \times g \times v^2 \times n^2}{h^{(\frac{1}{3})}}$$

Where:

$\tau_{b,cell}$ = Steady state bed shear stress (Pa)

ρ = Density of water (1000kg/m^3)

g = Acceleration due to gravity (9.81m/s^2)

v= Magnitude of velocity (m/s)

n= Manning's roughness (unitless)

h= Cell depth (m)

Results

Model Calibration and Evaluation

Calibration to the observed streamflow (Q)-WSE relationship yielded best-fit roughness values of 0.05, 0.45 and 0.04 for the channel, floodplain, and access path respectively. The fully calibrated model produced a RMSE of 5.6cm with all modeled flows falling within the 95th prediction interval of the collected data.

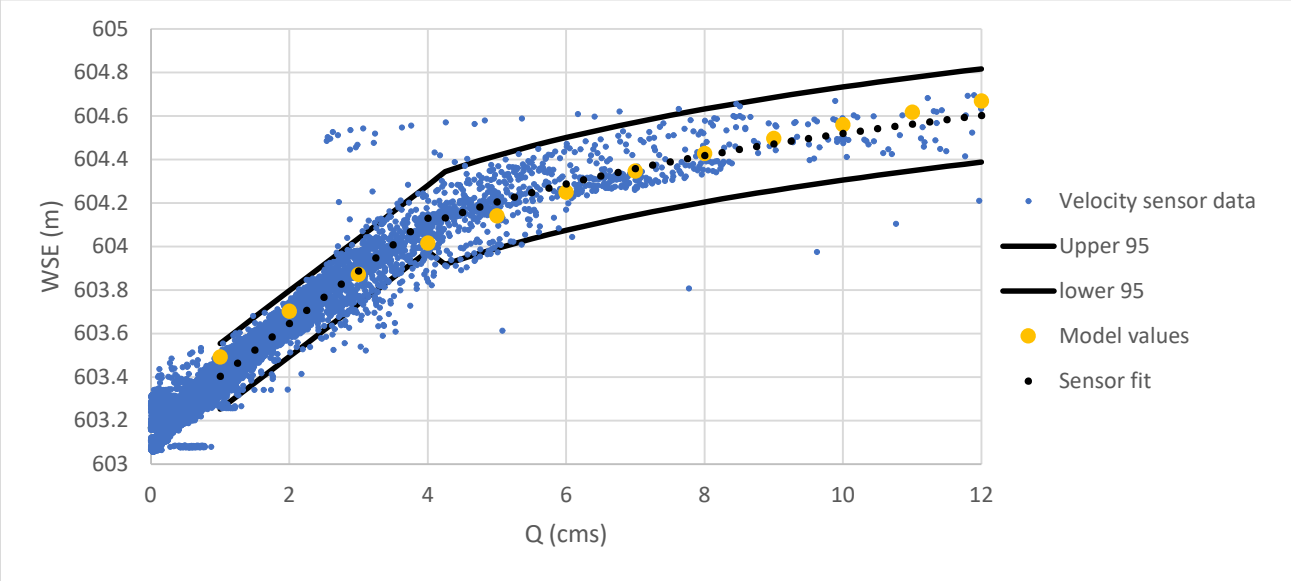

Figure 2: Calibrated model results, simulated streamflow (Q) and water-surface elevation (WSE) data compared to the observed data from the up looking ADCP at bridge 2.

The four evaluation runs of observed peak flows had a RMSE of below 10cm. These runs showed less accuracy than calibration runs, likely because of nonuniformity in roughness, which was constant in the model over the three zones. All four evaluation runs showed acceptable error with the RMSE of each run below values found in a similar 2-D HEC-RAS model of the same reach with more complex characterizations of roughness (Prior 2021).

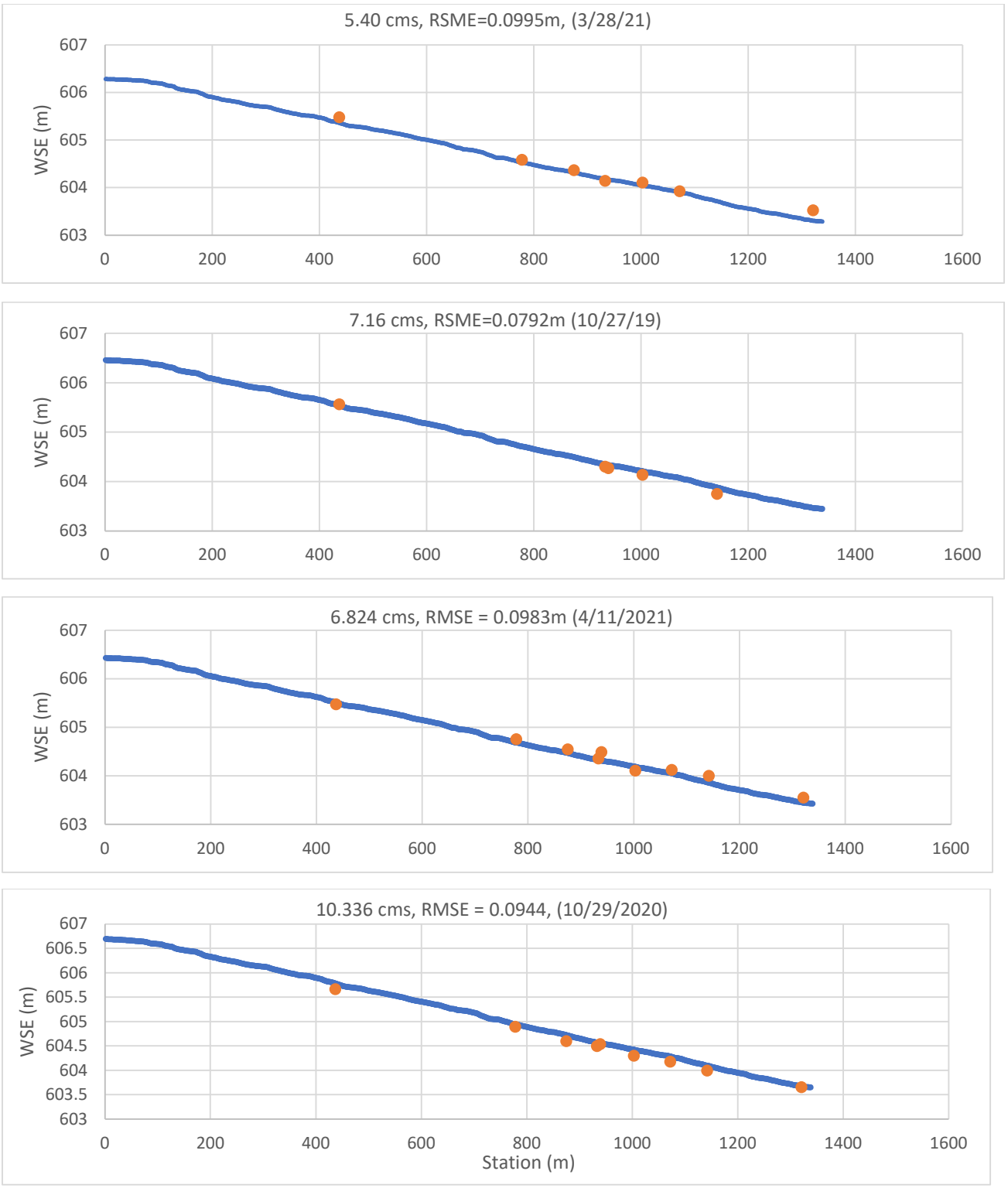

Figure 3: Simulated water surface profiles vs the observed water surface measurements.

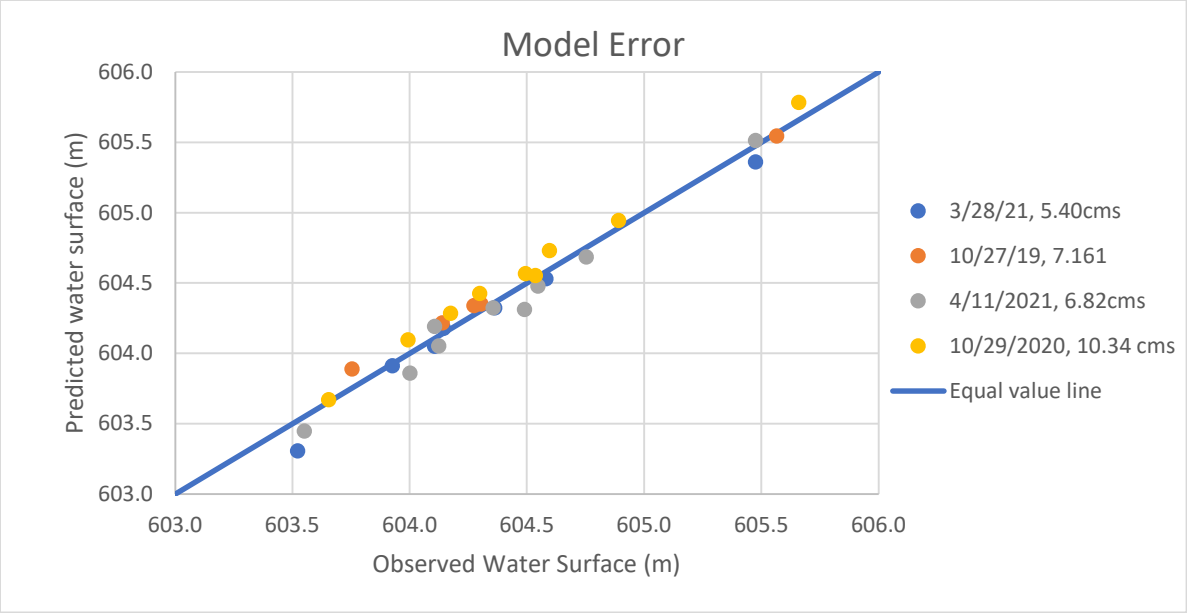

Figure 4: Differences between the predicted and observed water surfaces.

Floodplain Dynamics Characterization

Model simulation results revealed differences in floodplain morphology and water quantity. The highlighted insets to the right of the full site map show representative portions of each treatment depicting how the floodplains of each treatment became inundated. The first two insets showed portions of Treatment 1 which have long depressions and convey flow during floods. This was best seen in the 3 cms flow as these channels are just being inundated. These floodplain channels were most numerous and the most well defined in Treatment 1, but some more poorly defined features existed in the regraded reaches. It was observed that these floodplain channels usually spanned one meander length and brought water out onto the floodplain before it quickly returned to the main channel. A longer set of poorly defined channels on the western floodplain were seen at the 12 cms flow in Treatment 2. Shallow chute cutoff channels were also seen in the inset floodplain of Treatment 3. These were not as well defined or as deep as those observed in Treatment 1.

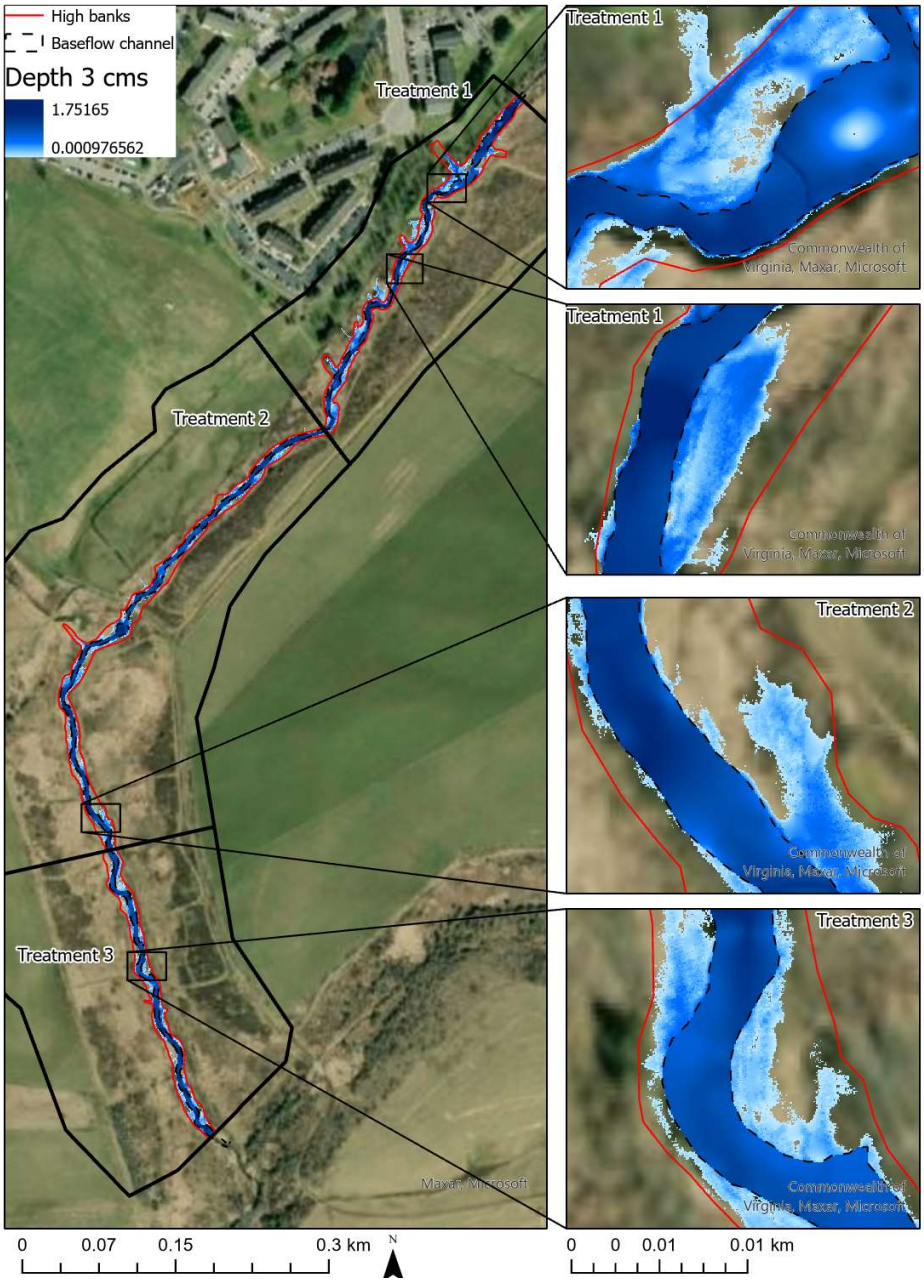

Figure 5: Simulated depths at 3cms. Key areas are highlighted to show how the floodplains of each treatment become inundated with increasing magnitude flows.

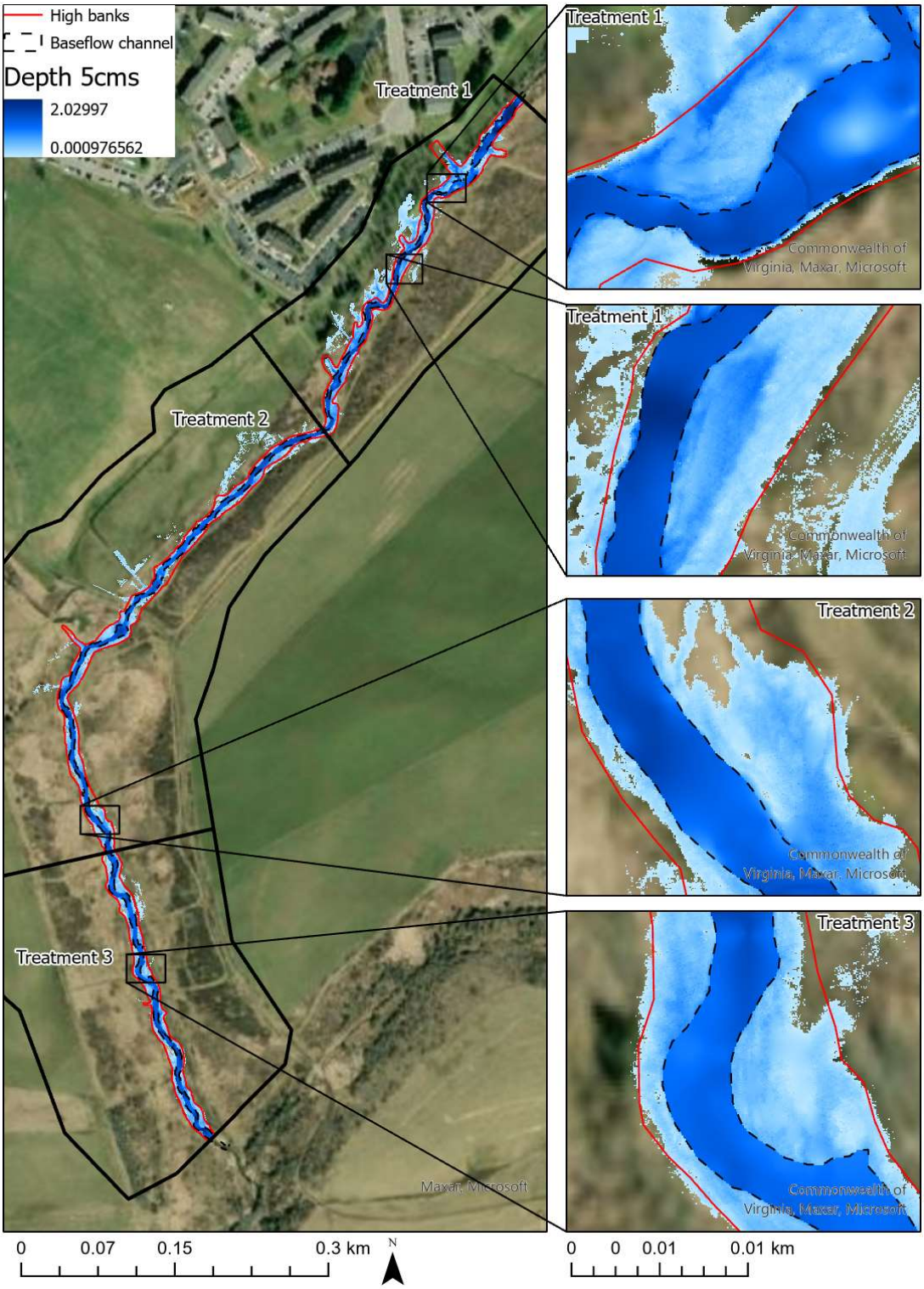

Figure 6: Simulated depths at 5cms. Key areas are highlighted to show how the floodplains of each treatment become inundated with increasing magnitude flows.

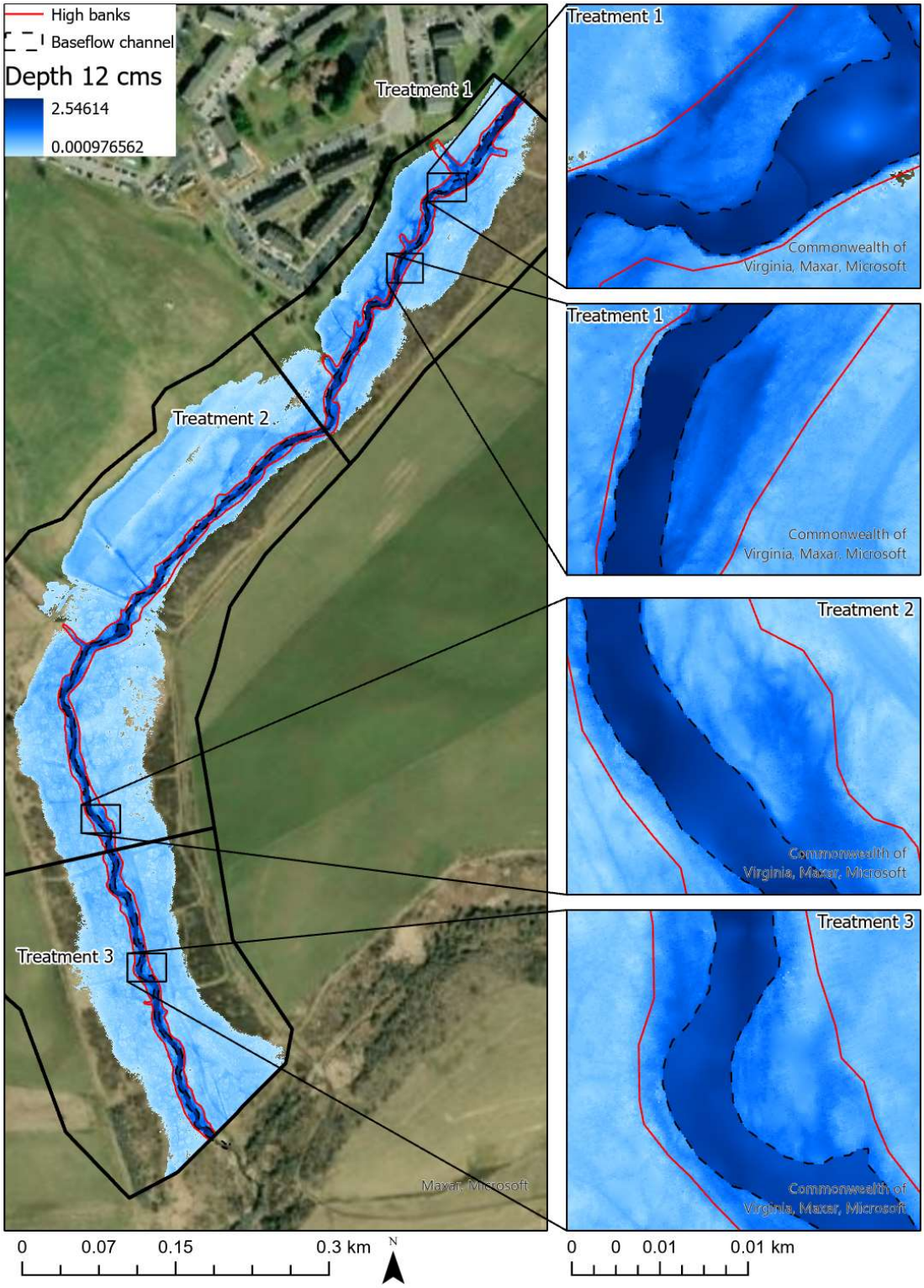

Figure 7: Simulated depths at 12cms. Key areas are highlighted to show how the floodplains of each treatment become inundated with increasing magnitude flows.

The normalized volume of water in the floodplain was higher in Treatment 1 than in either regraded treatment for lower magnitude flows (below 7cms; Figure 8). At these lower magnitude flows the difference between Treatments 1 and 3 was greatest at 3 cms where Treatment 1 had 29% higher normalized volume than Treatment 3. For flows above 7 cms the floodplain volume was highest for Treatment 3, followed by Treatment 1 and then Treatment 2. The largest difference in normalized floodplain volume between Treatment 3 and 1 in these higher flows was experienced at 12 cms where Treatment 3 had 4% higher floodplain volume.

When the inset floodplain was excluded from calculations of floodplain volume, the relationship changed significantly. Considering the inset floodplain best represents the overall floodplain dynamics of the system, but considering the dynamics of only the upper floodplain can help up see some additional nuance in the system. The normalized volume of Treatment 1 was highest for the lower magnitude flows and reached a maximum of 75% more volume in the floodplain than Treatment 3. At these flows the differences between Treatments 2 and 3 were much smaller than the differences between their full floodplain normalized volume. During high flows (6.5-12 cms) the relatively high floodplain volume was higher for both active treatments with the maximum difference occurring at 12 cms with a difference of 17% between Treatments 1 and 2 and 13% between Treatments 1 and 3.

a) **b)**

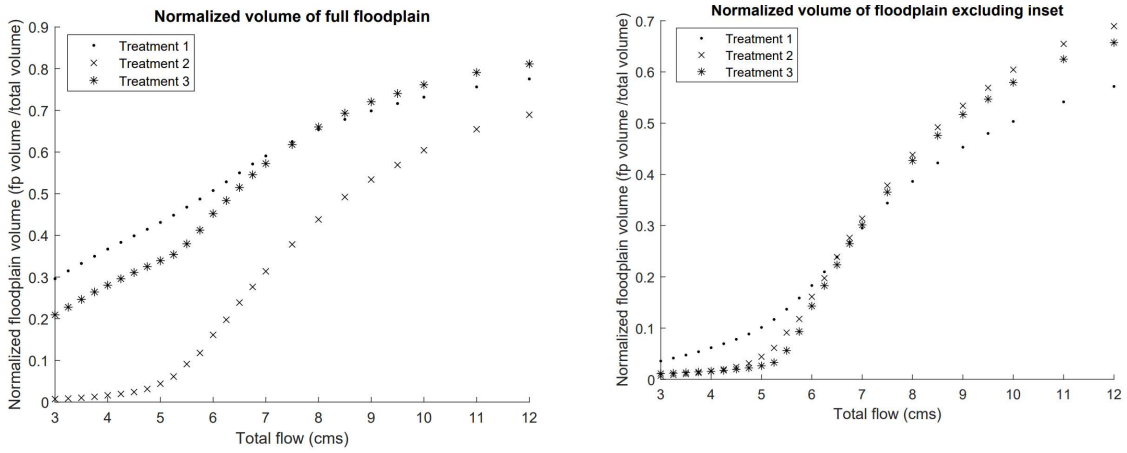

Figure 8: Normalized water volume of floodplain for all treatments (floodplain volume/channel volume), including (a) and then excluding (b) the inset region in floodplain volume calculations.

The average flooded top width of the passive treatment was shown to be the highest of any treatment during moderate floods, but smallest for the largest floods (Figure 9). This highlights differences in floodplain morphology, namely a low-lying inset floodplain with a narrower main valley in Treatment 1. Treatment 2 and 3 have similar geometries with Treatment 3 having a smaller main valley.

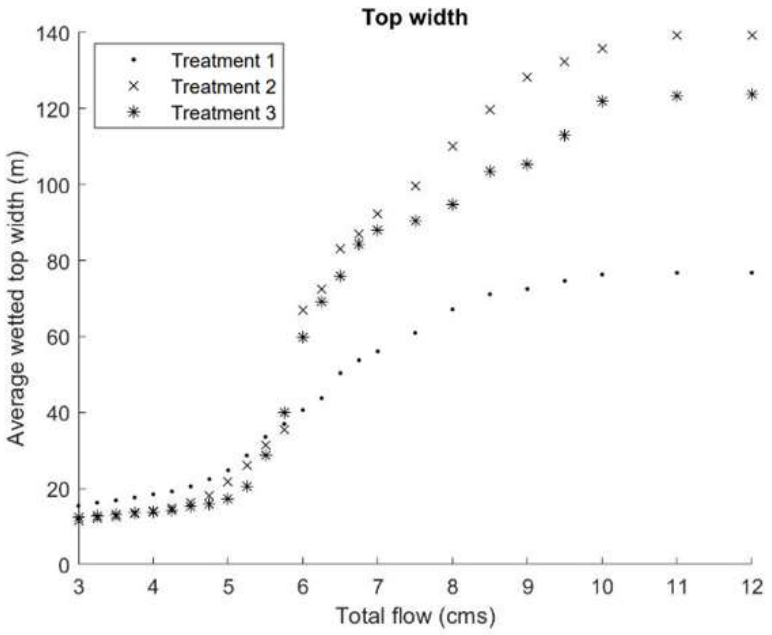

Figure 9: Wetted top width for the passive and active restorations.

Channel depth was highest in Treatment 1, followed closely by Treatment 3 with Treatment 2 having the lowest average depth (Figure 10). This highlights the influence of floodplain roughness in Treatment 1 where depths are greatest despite higher slope. In treatment 1 the low-lying floodplains begin inundation during small floods. The extra roughness of these floodplains likely contributes to the increases in water depth observed.

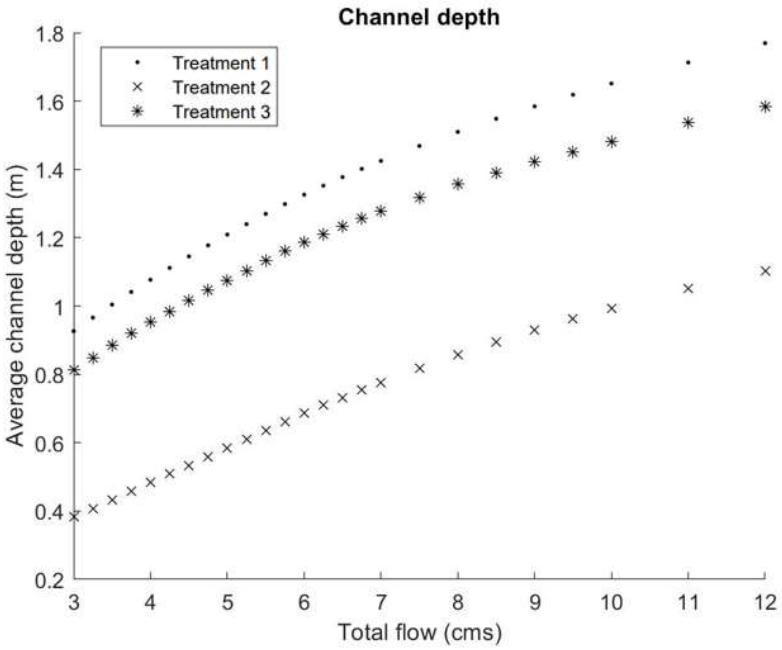

Figure 10: Average channel depth for each restoration at each modeled flow.

Channel velocities were significantly higher in treatment 1 than in either active treatment (Figure 11). This is likely due to the higher slope in treatment 1. The slope here is 0.3%, which is significantly higher than the slope in treatment 2, 0.2%. Interestingly the velocities in treatment 3 are nearly the same as observed in treatment 2. Here there is a smaller difference in slope, but the difference was still expected to create larger differences in velocity than was observed.

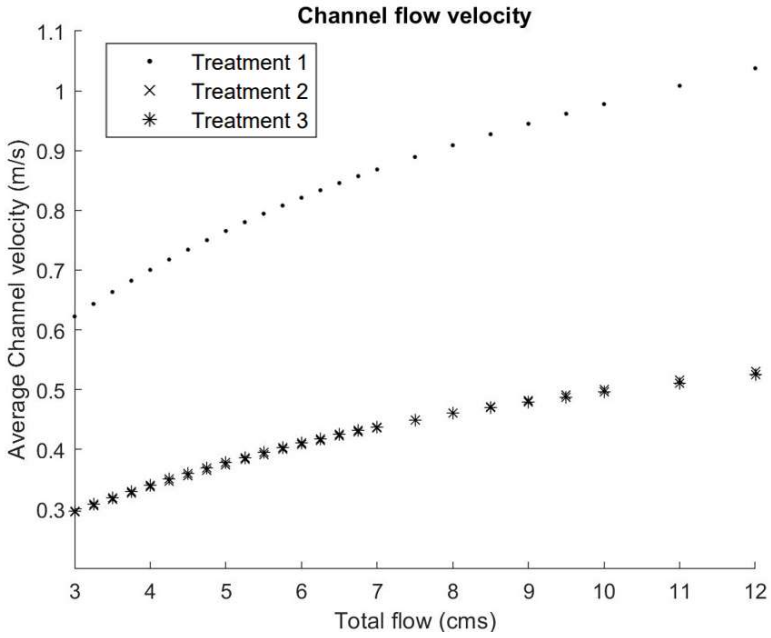

Figure 11: Average channel velocity for each restoration at each modeled flow.

Model results showed significantly higher channel-floodplain exchange for the passive restoration (Treatment 1) compared with the two active treatments (Treatments 2 and 3). The differences between the treatments increased with increasing discharge. This modeled difference became as high as 84% more exchange for Treatment 1 compared to Treatment 2 and 209% higher than to Treatment 3.

a) **b)**

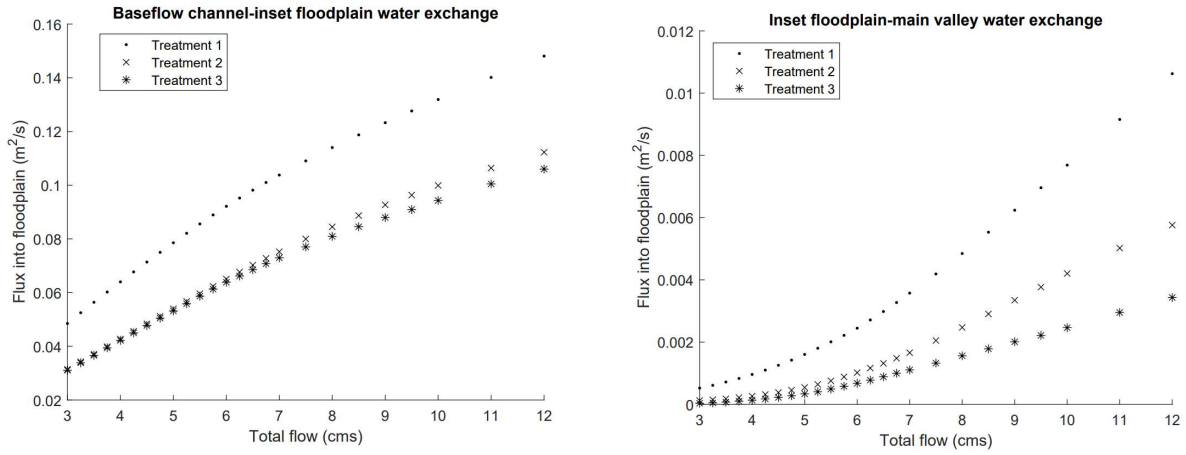

Figure 12: Channel-floodplain exchange between passive and active restorations, evaluated at the banks of the baseflow channel (a) and at the higher terrace (b).

Residence time for all treatments was significantly higher in the high floodplain than for the inset floodplain (Figure 13). The residence time generally increased with increasing flow except for the flows in Treatment 3 from 3-5 cms. Both active restoration treatments had higher residence times than the passive treatment except for the Treatment 2 inset floodplain at flows below 5cms. This difference was higher when excluding the inset floodplain from calculation of residence time. When considering the whole floodplain, residence time was very similar until 6.5 cms when the residence time for the actively restored treatments began to increase more quickly than that of the passively restored treatment. These diverging residence times have a maximum difference of 61% at 12 cms. This difference is likely to increase further at higher flows.

a) **b)**

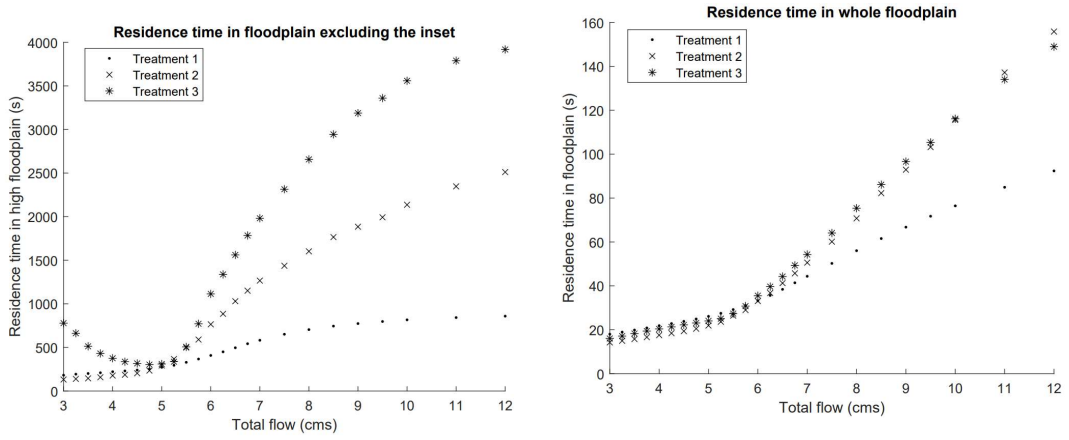

Figure 13: Floodplain water residence times for the high floodplain (a) and the inset floodplain (b) for each treatment.

Treatment 1 had the highest portion of its flow in the floodplain. Treatment 3 had floodplain flow comparable with Treatment 1 and Treatment 2 had significantly less than either. The differences between Treatments 1 and 3 were largest for moderate floods. Treatment 2 shows no increase in floodplain discharge until 7 cms when it increases at approximately the same rate as Treatments 1 and 3. At the highest flows, Treatments 1 and 3 have almost double the flow in their respective floodplains compared to Treatment 2.

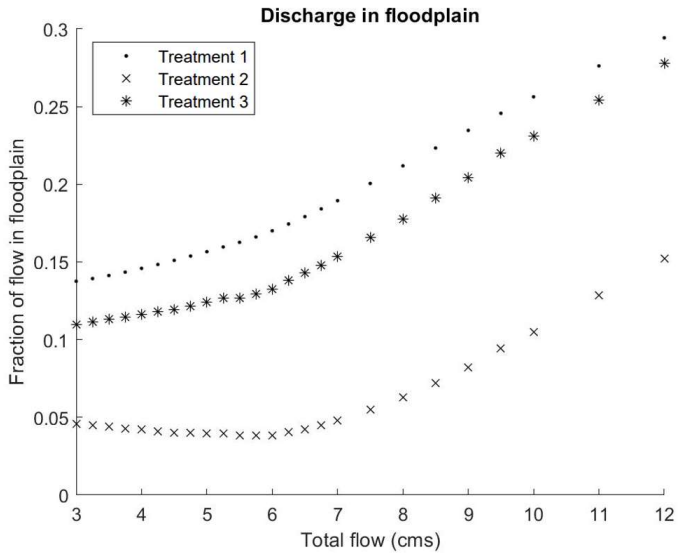

Figure 14: Average fraction of total flow conveyed in the floodplain of each treatment.

Shear Stress Analysis

The average channel shear stress for both active treatments were lower than those modeled for the passive treatment. Treatment 2 had the lowest average bed shear stress, up to 34% lower than the passive treatment. Treatment 3 experienced less average channel shear stress of up to 26% compared to the passive treatment. The modeled maximum channel shear stress was lowest for site 3 with reductions of up to 24%. This difference was highest at a flow of 5.5cms which is just above the flow which fully inundated the inset floodplain. The treatment at Treatment 2 had reductions in maximum channel shear stress for flows up to 7cms but had higher shear stresses at flows above that threshold. These high shear stresses were concentrated just downstream of a major constriction at a bridge which spans the baseflow channel. This treatment had shear stresses which were up to 6% higher than those modeled for Treatment 1 but provided reductions in maximum channel shear stress of up to 22% for lower flows.

a)

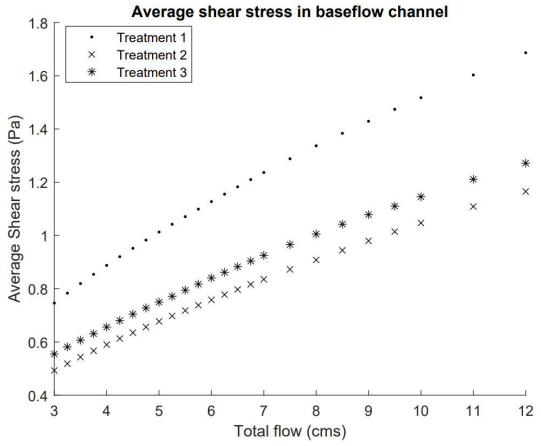

b)

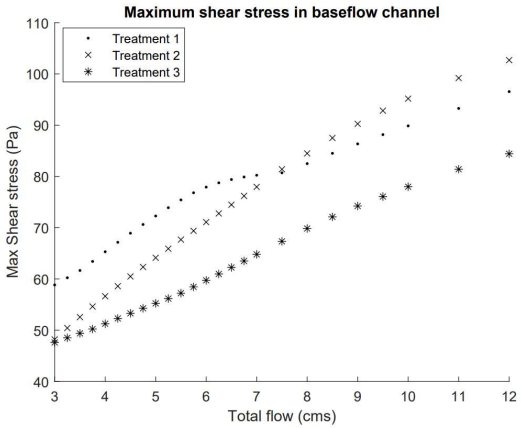

Figure 15: Average (a) and max bed shear stresses (b) modeled in the baseflow channel of each restoration.

Discussion

Model results showed that the passive treatment (1) has formed more highly connected floodplain channels in the inset and main floodplain compared to the active treatments (2 and 3). It is hypothesized that the more variable bank and floodplain geometry of these floodplain channels formed in Treatment 1 because of the lack of bank stabilization. Without stabilization the stream can make more rapid adjustments leading to the higher sinuosity observed and form more complex floodplain structures. These floodplain channels convey flow from the main channel and transport it from one meander bend to the next, causing high exchange rates and low floodplain residence times. This can also be seen in Figure 12 which shows that Treatment 1 has the highest fraction of flow in the floodplain. Results indicate that the lower lying

floodplain channels of Treatment 1 lead to higher exchange than either regrading treatment provided.

Floodplain channels have previously been shown to cause high rates of mass exchange (Czuba et al., 2019). Floodplains with channels were found to relieve the main channel of flow during moderate floods as did the floodplain channels observed in Treatment 1. Practitioners may be able to use this property of floodplain channels to design restoration solutions which preserve or enhance the action of floodplain channels. This would mimic natural streams by adding flow paths though the floodplain and relieving the baseflow channel at moderate floods as observed by Lindorth et al (2020). A concern of these floodplain channels is that they can be net erosional (Sumaiya et al. 2021) or depositional depending on their geometry and influent sediment load. This is of particular concern for the study site as it is impaired for excess fine sediment loading and any errosion could contribute sediment to the stream. Larger floodplains have been shown to have floodplain channels which can be depositional depending on the sediment loading and geometry (Lewin, 2017). The floodplain structures of this system have not been characterized as net erosional or depositional, further research is needed to make this distinction and quantify the impact stabilization has had on the sediment loading contribution from bank erosion.

The floodplains of Treatment 3 did show higher inundation than the floodplain of Treatment 2 but had lower volume in the floodplain compared to Treatment 1 at lower flows (Figure 8). These data suggest that Treatments 2 and 3 were both worse at connecting the channel with the floodplain in smaller floods than the natural channel evolution of Treatment 1. At higher flows the normalized floodplain volume of Treatment 3 overtakes that of Treatment 1

(Figure 8). This may be due to the wider main valley of Treatment 3. This leads to Treatment 1's floodplain becoming full while Treatment 3 continues to fill.

Formation of inset floodplains and floodplain channels was likely impeded by the streambank stabilization measures implemented in the active restoration treatments in Treatment 2 and 3. This retardation is best seen in Treatment 2, where sinuosity is lowest, contributing to the lack of channel-floodplain exchange as there are fewer meanders to facilitate cross meander flow. The creation of the inset floodplain in Treatment 3 minimizes this impact of stabilizing a straight reach by allowing for engineering of small meanders through adjusting the position of the inset floodplain along the longitude of the channel. Regrading area only outside the baseflow channel removes the possibility of engineering in sinuosity, locking the channel in its current straight form instead of one with a higher engineered sinuosity. This restoration is contrasted well by Hammersmark et al.'s (2008) findings on pond and plug restoration. This form of restoration adds meander bends and intentionally decreases channel capacity. Modeling of as built conditions in such restorations showed increases in floodplain volume. Notably, Hammersmark's study did not allow time for channel adjustment before analysis. It has not been shown how long this reconnection is maintained.

Though Treatment 1 had higher channel-floodplain exchange than either active treatment (2 and 3), this did not lead to decreases in bed shear stresses. Instead, both active treatments had lower average channel bed shear stress for all modeled flows. Difference in longitudinal slope may cause the difference in bed shear stress rather than decreases brought by regrading. The treatments with higher slopes had the highest bed shear and bed shear stress

is directly proportional to bed slope (Garcia 2008). The work of McKean et al. (2013) has shown that floodplain access can reduce the bed shear stress of larger rivers.

The highest shear stresses experienced were in Treatment 2 just downstream of a major constriction caused by a concrete bridge. This concrete bridge and associated road fully impede flow in the floodplain at all modeled flows, restricting all flow to the baseflow channel which causes high velocities and shear stresses which have carved out a wide, deep pool on the lee side of the bridge.

The high connectivity of the passive treatment is thought to be due to channel adjustment, but this adjustment means that the channel substrate has been reworked. For streams which have fine sediment load impairments understanding the sediment balance of this passive reworking is essential to deciding how to manage these systems. Additional studies of historical cross sections of the stream could be used to make estimates of bank sediment load in the stream. By considering the sediment contribution of the adjusting bank in the passive treatment a more wholistic view of how passive management impacts the system would further educate decisions to regrade streams. Additional studies should also investigate the unsteady flow attenuation of each treatment. The higher connectivity of the passive treatment suggests that it would attenuate peak flows better than the other two sections, but an unsteady flow model could shed light on this property more concretely.

Conclusions

Regrading banks to lower slopes, as seen in Treatment 2, produced the lowest channel-floodplain connectivity by all metrics. The bank stabilization in this treatment held the form of

the previously straightened channel, preventing formations of inset floodplains or meander bends which formed more readily in treatments where the channel was allowed to evolve. Adding an inset floodplain provided better channel-floodplain connectivity than just regrading the bank slopes by all metrics, but how it compares with the passive treatment is less clear. Some metrics of floodplain connection and bed stability indicated that the engineered inset floodplain was better connected with the channel than that which formed in Treatment 1, while other metrics indicated the opposite. The flow moving though the floodplain, flood floodplain volume, and channel-floodplain exchange were highest for Treatment 1 while Treatment 3 had the lowest R_{eff} and highest floodplain volume during the largest flood events. Overall, the high connectivity of the passive treatment suggests that stabilization through regrading does not provide additional connectivity. By this metric, the cost of in place stabilization is unjustifiable. Practitioners should instead attempt to influence stream function with passive techniques such as cattle removal and replanting.

References

Bernhardt, E., et al. **2005**. Synthesizing U.S. river restoration efforts. Science, 308, pp. 636-637 https://doi.org/10.1126/science.1109769

Bernhardt, E., Palmer, M. 2011. River restoration: the fuzzy logic of repairing reaches to reverse catchment scale degradation. Ecological Applications, vol. 21, No. 6

Booth, D., Fischenich, C. **2015**. A Channel Evolution model to guide stream restoration. Area vol. 47 issue 4 p. 408-421 https://doi.org/10.1111/area.12180

Byrne, C., Stone, M., Morrison, R. **2019**. Scalable Flux metrics at the Channel-floodplain Interface as Indicators of Lateral Surface Connectivity. Water Resources Research vol 55 issue 3 **https://doi.org/10.1029/2019WR026080**

Czuba, J., David, S., Edmonds, D., Ward, A., **2019**. Dynamics of Surface-Water Connectivity in a Low-Gradient Meandering River. Water Resources Research vol 55 issue 3 p. 1849-1870 **https://doi.org/10.1029/2018WR023527**

García, M. H. **2008**. Sedimentation engineering: processes, measurements, modeling, and practice. Reston, Va.: American Society of Civil Engineers.

Hammersmark, C., Raines M., Mount, J., **2008**. Quantifying the hydrological effects of stream restoration in a montane meadow, northern California, USA https://doi.org/10.1002/rra.1077

Laub, B., et al. **2013**. Comparison of Designed Channel Restoration and Riparian Buffer Restoration Effects on Riparian Soils. Restoration Ecology vol 21 issue 6. https://doi.org/10.1111/rec.12010

Levell, A., Chang, H., **2008.** Monitoring the channel process of a stream restoration project in an urbanizing watershed: a case study of Kelley Creek, Oregon, USA. River Reach Applications, vol 24 issue 2. https://doi.org/10.1002/rra.1050

Lewin, J., Ashworth, P. J., & Strick, R. J. P. (2017). Spillage sedimentation on large river floodplains. *Earth Surface Processes and Landforms*, **42**(2), 290– 305. https://doi.org/10.1002/esp.3996

Lindworth, E., Rhoads, B., Castillo, C., Czuba, J., Güneralp, I., Edmonds, D., **2020.** Spatial Variability in Bankfull Stage and Bank Elevations of Lowland Meandering Rivers: Relation to Rating Curves and Channel Planform Characteristics. Water Resources Research, vol 56, issue 8. **https://doi.org/10.1029/2020WR027477**

McMillan S. **2017**. Increasing floodplain connectivity through urban stream restoration increases nutrient and sediment retention. Ecological Engineering vol 108a. https://doi.org/10.1016/j.ecoleng.2017.08.006

McKean J, Tonina D. **2013**. Bed stability in unconfined gravel bed mountain streams: With implications for salmon spawning viability in future climates. J Geophys Res Earth Surf. 118. doi:10.1002/jgrf.20092

National Oceanic and Atmospheric Administration **2021**. Online Positioning User Service. https://www.ngs.noaa.gov/OPUS/

Prior, E.M.; Aquilina, C.A.; Czuba, J.A.; Pingel, T.J.; Hession, **2021.** W.C. Estimating Floodplain Vegetative Roughness Using Drone-Based Laser Scanning and Structure from Motion Photogrammetry. Remote Sens. 2021, 13, 2616. https://doi.org/10.3390/rs13132616

Rubin, Zan, G. M. Kondolf, and Blanca Rios-Touma. **2017**. "Evaluating Stream Restoration Projects: What Do We Learn from Monitoring?" *Water* 9, no. 3: 174. https://doi.org/10.3390/w9030174

Wynn, T.; Hession, W.C.; Yagow, G. Stroubles Creek Stream Restoration, Final Project Report; Virginia Department of Conservation and Recreation: Richmond, VA, USA, 2010; pp. 1–19.

Trimble, S. **1994**. Erosional effects of cattle on streambanks in Tennessee, U.S.A. Earth surface processes and Landforms, vol 19 issue 5, p. 451-464 https://doi.org/10.1002/esp.3290190506

Wohl, E., S. N. Lane, and A. C. Wilcox **2015.** The science and practice of river restoration, Water Resour. Res., 51, 5974–5997, https://doi:10.1002/2014WR016874

Worley, L., Underwood, K., Vartanian, N., Dewoolkar, M., Matt, J., Rizzo, D., 2022. Semi-automated hydraulic model wrapper to support stakeholder evaluation: A floodplain reconnection study using 2D hydrologic engineering center's river analysis system. River Research and Applications 0 (0) 1535-1459 https://doi.org/10.1002/rra.3946

Sholtes, J. **2009**. Hydraulic analysis of stream restoration on flood wave propagation. The University of North Carolina at Chapel Hill. ProQuest Dissertations Publishing, 2009. 1467299. https://doi.org/10.17615/s1ag-v630

Sumaiya, S., Czuba, J., Schubert, T., David, S., Johnston, G., Edmonds, D., **2021**. Sediment Transport Potential in a Hydraulically Connected River and Floodplain-Channel System. Water Resources Research vol 57, issue 5. **https://doi.org/10.1029/2020WR028852**

U.S. Geological Survey, 2021. 20210629, USGS 1 Meter 17 x54y412 VA_FEMA-NRCS_SouthCentral_2017_D17: U.S. Geological Survey. https://www.sciencebase.gov/catalog/item/60ddf580d34e3a6dca28a0f7